Rydberg-atom acceleration by tightly focused intense laser pulses

P. Cai,[1] J. J. Zha,[1] Y. J. Xie,[2] Q. Wei,[3,*] and P. X. Wang[1,†]

[1]*Key Laboratory of Nuclear Physics and Ion-Beam Application (MOE), Institute of Modern Physics, Department of Nuclear Science and Technology, Fudan University, Shanghai 200433, China*

[2]*Joint Service College, National Defense University, Beijing 100858, China*

[3]*State Key Laboratory of Precision Spectroscopy, East China Normal University, Shanghai 200062, China*

(Received 27 January 2019; published 1 May 2019)

Recent experiments and simulations have shown that pulsed lasers can be used to push neutral Rydberg atoms forward or pull them back toward a light source. Referring to an earlier experiment [U. Eichmann *et al.*, Nature **461**, 1261 (2009)], we simulate both pushing and pulling effects on ^{1}H and ^{12}C in tightly focused laser fields with a high-order corrected optical description. Scaling laws of excited ^{4}He acceleration by laser pulses are investigated via numerical simulations, which show that Rydberg atoms can be pushed or pulled to high speeds even up to hundreds of kilometers per second by tightly focused laser pulses. Moreover, we use the ponderomotive model and computer simulation to further analyze the validity of two formulas of the maximum radial and longitudinal velocity of outgoing accelerated Rydberg atoms. These studies have practical guiding significance to laser-based acceleration of neutral particle experiments in laboratories.

DOI: 10.1103/PhysRevA.99.053401

I. INTRODUCTION

Acceleration of neutral particles is very important in many areas [1–3]. However, compared to charged particles, it is very difficult to accelerate a neutral particle. Recently, the acceleration of neutral particles has been widely studied experimentally [4–10], and many acceleration mechanisms have been adopted. Among them, a physical acceleration mechanism is the exciting of atoms to Rydberg states in an intense laser field, and subsequently using ponderomotive force experienced by the excited electron [11–13] to drag the inner core by means of the Coulomb force between them [14]. In addition to the ponderomotive potential, there exists a smaller term that comes from the binding energy of the Kramers-Henneberger (KH) atom [15]. Our recent study shows that including this KH term brings the calculated maximum velocities to a close match with experimental results over the entire duration of the laser pulse [16]. However, the contribution from the KH term is less than 5% of that from the ponderomotive force, and this proportion will decline with increase in laser field intensity and the laser wavelength. Hence, we use the ponderomotive model for analysis and simulations [4]. To simulate Rydberg atoms accelerated in a tightly focused laser field, an optical description with high-order corrections is taken into account.

II. ASSUMPTIONS AND MODEL

If $a(r,t) \ll 1$ ($a \equiv qE/m\omega c$, where E is the magnitude of the electric field; q and m are the particle charge and mass, respectively; c is the speed of light in vacuum; and ω is the angular frequency of the electromagnetic wave), i.e., the optical intensity is not very high, the ponderomotive potential experienced by a particle can be written as [17]

$$U'_{\text{pond}} \approx \frac{a(\mathbf{r},t)^2}{4} mc^2. \tag{1}$$

Then the force felt by the neutral Rydberg atom can be regarded as mainly coming from the excited electron's ponderomotive force, and we can get [4,17]

$$\begin{aligned}\mathbf{F}_{\text{pond}}(t) &= -\nabla U'_{\text{pond}} = (M + nm_e)\ddot{R}(t) \\ &\approx -\frac{e^2}{4m_e\omega^2}\nabla|E_0(\mathbf{r},t)|^2,\end{aligned} \tag{2}$$

where $\ddot{R}(t)$ is the center-of-mass position of the atom; the two dots represent the second-order derivative over time; M and m_e are the mass of the atomic nucleus and the mass of the electron, respectively; and n is the electron sum of the atom.

In a strong laser field, for a loosely bound electron in a Rydberg-state atom, the electron is quasifree [4]. Thus, we do not distinguish between different Rydberg states in our calculation. After Rydberg atoms act with the laser pulse, they fly to the detector in the free space. These Rydberg atoms can be regarded as independent of each other, and their interaction is not considered. Figure 1 presents the schematic geometry of neutral atoms interacting with laser pulses. The excitation of an atom may occur anywhere in the laser pulse. (x_0, y_0, z_0) represents the position of the excitation, and Z_L presents the instantaneous peak position of the laser pulse along the z direction. Then the relative position of the excitation in the laser pulse along the z direction is $\Delta Z = z_0 - Z_L$.

*qwei@admin.ecnu.edu.cn
†wpx@fudan.edu.cn

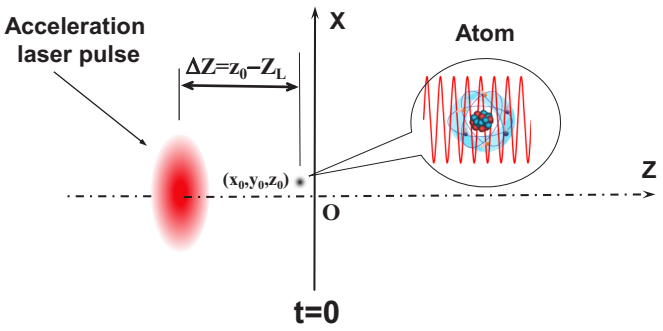

FIG. 1. Schematic geometry of neutral atoms interacting with laser pulses.

The intensity of the laser pulse with paraxial approximation can be expressed as

$$I(\mathbf{r},t) = |E_0(\mathbf{r},t)|^2 = a_0^2 \frac{w_0^2}{w(z)^2} \exp\left[-\frac{2r^2}{w(z)^2}\right] f(\eta), \quad (3)$$

$$w(z) = w_0[1 + (z/Z_R)^2]^{1/2}, \quad (4)$$

$$\eta = ct - z, \quad (5)$$

where $a_0 = eE_0/m\omega c$ is the magnitude of the field intensity at the center of the laser focus, $f(\eta) = \exp[-(\eta/c\tau)^2]$ is a Gaussian time envelope profile of the optical intensity, $Z_R = kw_0^2/2$ is the Rayleigh length, k is the wave number, and w_0 is the beam waist. We can expand Eq. (5) in Ref. [4] for the ^{4}He atoms excited at different positions r (perpendicular to the laser beam direction) in the focus plane to obtain [4]

$$v_\perp = \frac{e^2 I_0 r}{1.33 \times 10^{-3} M m_e \omega^2 w_0^2} \exp\frac{-2r^2}{w_0^2} \sqrt{\pi}\tau, \quad (6)$$

where $\tau = \tau_{\mathrm{FWHM}}/(2\sqrt{\ln 2})$, τ_{FWHM} is the full width at half maximum of the intensity of the laser pulse, and I_0 is the intensity of the laser focus center.

To get Eq. (5) in Ref. [4], the atom is assumed to be in the Rydberg state before it interacts with the laser pulse ($\Delta Z \sim \infty$). This assumption seems unreasonable because an atom can be excited only after interaction. In fact, our simulation results of the radial outgoing velocity of the excited atoms for larger values of ΔZ (such as $\Delta Z = 2c\tau$) is almost the same as that for $\Delta Z \sim \infty$. Thus, it is reasonable to assume that the atom is in the Rydberg state long before the laser pulse arrives; i.e., $\Delta Z \sim \infty$.

The ponderomotive force is proportional to the gradient of the laser field. Therefore, a laser pulse with a small waist favors ponderomotive acceleration because a small beam waist corresponds to a large field gradient. However, the paraxial approximation of the field is not accurate enough for a tightly focused laser pulse (very small beam waist) [18]. To obtain a higher final outgoing velocity in a tightly focused laser pulse, we use an optical field description with high-order corrections. Using the ponderomotive model, we require only the amplitude distribution of the total electric field, which is the same as that of the vector potential. The high-order corrected vector potential for a monochromatic fundamental linearly polarized Gaussian beam with a long pulse length is given as [18]

$$A(\mathbf{r},t) = a_0 f_0(\eta)(\Lambda_0 + \varepsilon^2\Lambda_2 + \varepsilon^4\Lambda_4 + \cdots)e^{-i\varsigma/\varepsilon^2 + ikct + i\phi_0}, \quad (7)$$

$$\Lambda_0 = iQ\exp(-i\rho^2 Q) \quad (8)$$

$$\Lambda_2 = (2iQ + i\rho^4 Q^3)\Lambda_0, \quad (9)$$

$$\Lambda_4 = (-6Q^2 - 3Q^4\rho^4 - 2iQ^5\rho^6 - 0.5Q^6\rho^8)\Lambda_0, \quad (10)$$

where $\varsigma = z/(kw_0^2)$, $\xi = x/w_0$, $\zeta = y/w_0$, $\varepsilon = 1/(kw_0)$, $\rho^2 = \xi^2 + \zeta^2$, and $Q = 1/(i + 2\varsigma)$. ϕ_0 is the initial phase of the field and $f_0(\eta) = \exp[-(\eta/c\tau_0)^2]$ is a Gaussian time envelope profile of the electric field intensity with a finite pulse duration of $\tau_0 = \tau_{0\mathrm{FWHM}}/(2\sqrt{\ln 2}) = \sqrt{2}\tau$.

III. SIMULATION RESULTS

Referring to the experiments reported in [4,19], we selected our simulation parameters as $\omega = 0.056$ a.u. ($\lambda = 0.814\,\mu$m), $w_0 = 16\,\mu$m, $I_0 = 2.8 \times 10^{15}\,\mathrm{W/cm^2}$ ($a_0 = 0.0368$), and $\tau_{\mathrm{FWHM}} = 120\sqrt{2}$ fs[1] (corresponding to the full width at half maximum of the electric field $\tau_{0\mathrm{FWHM}} = \sqrt{2}\tau_{\mathrm{FWHM}} = 240$ fs). Here, we assume that the excited atom is initially stationary, and that the laser pulse is at the position $\Delta Z = 2c\tau_0$ before it has an impact on the atom. Simulations of the excited atoms at different positions show that the position of the largest final radial velocity is on the focal plane. Figure 2 shows the final radial velocity distributions of the excited ^{4}He atoms on the x axis. Figure 2(a) indicates that the final outgoing radial velocity increases as the beam waist of the laser pulse decreases. This is because the gradient of the laser field near the focus is inversely proportional to the waist of the laser pulse. Figure 2(b) indicates that the final radial velocity increases as the duration of the laser pulse increases, because a longer laser pulse denotes longer time of acceleration.

According to Eq. (6), a laser pulse with a long pulse duration and a small waist will favor ponderomotive acceleration. Figure 3 presents the variation of the final radial and longitudinal velocity with respect to the laser pulse length $\tau_{0\mathrm{FWHM}}$, where the dotted lines represent the results from Eq. (6) while the solid lines represent the simulation results. We observe that both results agree well in the condition of a relatively short pulse, while for a much longer pulse they show an obvious deviation. Normally, a longer laser pulse duration implies a longer acceleration time, and a decreasing laser intensity gradient, i.e., decreasing laser ponderomotive force. In addition, because of the transverse force, the atom may not keep being accelerated for long enough to leave the accelerated light field. Thus, if the laser pulse duration is very long (e.g., a continuous laser beam), it will have an adverse impact on ponderomotive acceleration. Figure 3 shows identical maximum outgoing velocities for particles with different pulse lengths and waists for a certain laser

[1]According to the results and formula (5) in Ref. [4], we conversely calculated that the laser pulse length in their experiment should be $\tau_{\mathrm{FWHM}} = 120\sqrt{2}$ fs but not $\tau_{\mathrm{FWHM}} = 120$ fs.

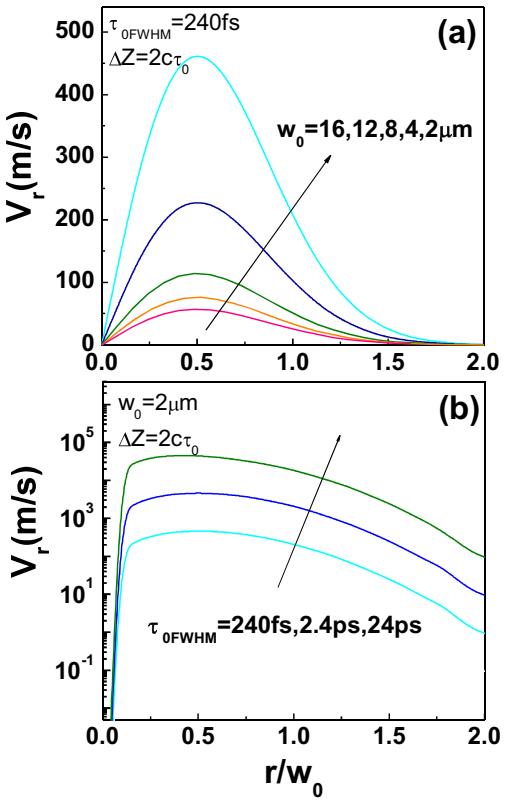

FIG. 2. Final outgoing radial velocity distribution of excited ^{4}He atoms at positions along the x axis, where the simulation parameters are $\Delta Z = 2c\tau_0$, and (a) $\tau_{0\mathrm{FWHM}} = 240$ fs, and $w_0 = 2,\ 4,\ 8,\ 12,\ 16\,\mu$m; (b) $w_0 = 2\,\mu$m, and $\tau_{0\mathrm{FWHM}} = 24$ ps, 2.4 ps, 240 fs. The other parameters are $I_0 = 2.8 \times 10^{15}$ W/cm^2 and $\lambda = 0.814\,\mu$m.

intensity, and the value of the maximum outgoing velocity is proportional to the laser intensity; however, the pulse length at an optimal acceleration decreases with decreasing waist. Hence, we can design an optimal acceleration scenario by

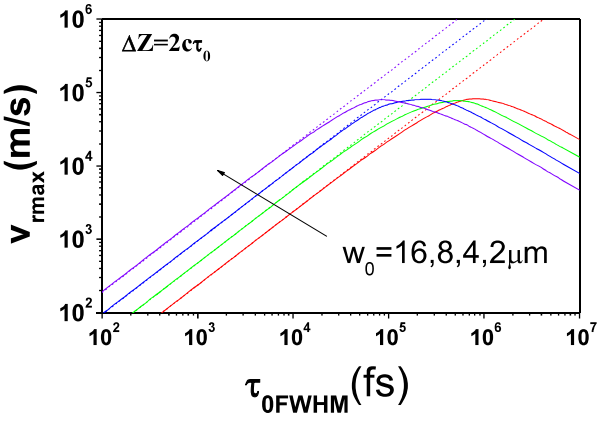

FIG. 3. Variation of the maximum outgoing radial speed $V_{r\,\max}$ of the excited ^{4}He atoms with respect to laser pulse length $\tau_{0\mathrm{FWHM}}$ (the full width at half maximum of the electric field) for $z_0 = 0$ and $\Delta Z = 2\tau_0$. The solid lines are for simulation results and the dotted lines for the results from Eq. (6). The other parameters are $I_0 = 2.8 \times 10^{15}$ W/cm^2; $w_0 = 16,\ 8,\ 4,\ 2\,\mu$m; and $\lambda = 0.814\,\mu$m.

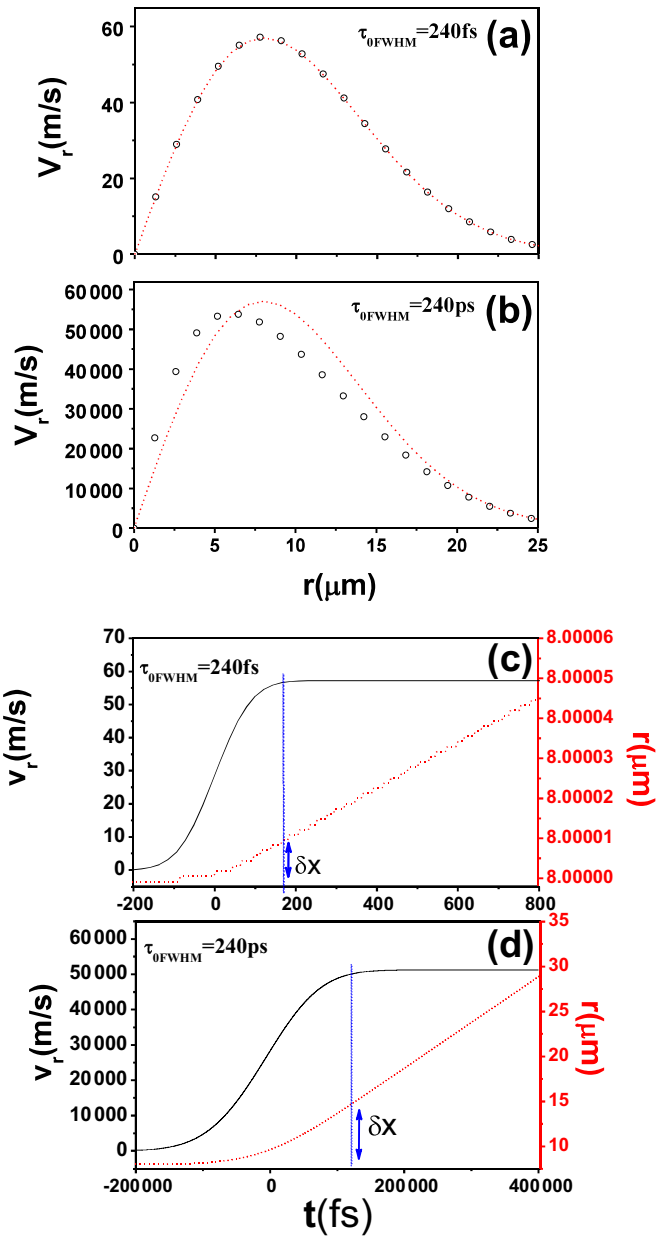

FIG. 4. Final outgoing radial velocity V_r distribution of excited ^{4}He atoms at positions along the x axis, where $\Delta Z = 2c\tau_0$. The dotted line is for the result from Eq. (6) and the circles are for the simulation results with $w_0 = 16\,\mu$m, $I_0 = 2.8 \times 10^{15}$ W/cm^2, $\lambda = 0.814\,\mu$m. (a) $\tau_{0\mathrm{FWHM}} = 240$ fs and (b) $\tau_{0\mathrm{FWHM}} = 240$ ps. The other simulation parameters are the same as in Fig. 2(a). (c) Radial velocity V_r (solid line) and the radial coordinate r (dotted line) of an excited ^{4}He atom as functions of the time t, where the excited ^{4}He atom located initially at rest at the position $(x_0 = w_0/2,\ y_0 = z_0 = \mathbf{0})$, where simulation parameters are the same as (a). (d) Same as (c) but with $\tau_{0\mathrm{FWHM}} = 240$ ps.

focusing and compressing the laser pulse to increase the laser intensity in the laboratory.

According to Eq. (6), the maximum radial acceleration (dotted line) at $z = z_0$ is obtained at half beam waist, $r = w(z_0)/2$, which is exactly the same as our simulation results (circles) when the laser pulse is ultrashort, as shown in Fig. 4(a). However, if the laser pulse is long enough (such

as $\tau_{0\mathrm{FWHM}} = 240\,\mathrm{ps}$), as shown in Fig. 4(b), our simulation results (circles) will deviate from those obtained using Eq. (6) (dotted line). The simulation results also show that the maximum radial acceleration at $z = z_0$ is not at half beam waist, and its value is less than that obtained with Eq. (6). Actually, the conclusion presented in Fig. 3 of Ref. [4] will not be valid for the case with a long laser pulse (such as $\tau_{0\mathrm{FWHM}} > 240\,\mathrm{ps}$); i.e., the maximum velocity transferred to the Rydberg atoms at the focal plane will not always increase linearly with respect to the laser pulse duration. Here, the problem is that Eq. (6) is based on the assumption that neutral atoms have no radial movement during the entire acceleration period, namely, $r(t) \equiv r$ [4]. Our simulation shows that this is true only when the laser pulse is ultrashort. As shown in Fig. 4(c), when $\tau_{0\mathrm{FWHM}} = 240\,\mathrm{fs}$, for the excited atom's radial movement $\delta r \sim 10^{-5}\,\mu\mathrm{m} \ll \lambda$ during the main acceleration stage, it is reasonable to assume $r(t) \equiv r$ for deriving Eq. (6). However, when $\tau_{0\mathrm{FWHM}} = 240\,\mathrm{ps}$, the excited atom's radial movement $\delta r \sim 8\,\mu\mathrm{m} \gg \lambda$ during the main acceleration stage, even larger than the half beam waist in the focus plane $w_0 = 16\,\mu\mathrm{m}$, as shown in Fig. 4(d); then it is invalid to assume $r(t) \equiv r$. A further analysis reveals that the position of particles for maximum radial acceleration on the focus plane is getting closer to the optical axis rather than at $r = w_0/2$ [as shown in Fig. 2(b)] and the position of particles for maximum radial acceleration along the z axis is not fixed on the focus plane when the pulse length is long enough. Figure 3 shows that when the pulse length increases to a certain value (e.g., $\tau_{0\mathrm{FWHM}} \sim 1$ ns), the maximum radial outgoing velocities of particles on the focus plane decreases with increasing pulse length. This is because during the interaction between the long laser pulse and particles, the latter will be pushed out of the optical field owing to the strong radial ponderomotive repulsive force acting before the peak position of the laser pulse arrives at the focus plane; thus, these particles cannot be well accelerated. This information is a useful tip for future laser-based acceleration experiments of neutral particles; in a word, we cannot expect to obtain arbitrary large radial outgoing velocities of neutral particles by increasing laser pulse length limitlessly.

Following we also assume that the excited atom is initially stationary. Simulations of the excited atoms at different relative positions show that the relative positions $\Delta Z = \mathbf{0}$, where maximum final longitudinal acceleration can be achieved, are obtained in all the cases. Simulation results in Fig. 5(a) reveal that the maximum longitudinal velocity of an atom is usually toward the light source when the laser pulse is short, thereby signifying that the atom is pulled backward by the laser. However, if the waist of the laser pulse is small enough (e.g., $w_0 = 2\,\mu\mathrm{m}$), the atom can gain a small velocity along the direction of the laser propagation when $z_0 > 0$. Figure 5(b) illustrates that when $\Delta Z = 0$, if the laser pulse is long enough, the atom may be pushed forward when $z_0 > 0$ and pulled backward when $z_0 < 0$. We use $V_{z\max}$ and $V_{z\min}$ to represent the maximum forward velocity [solid dots in Fig. 5(b)] and maximum backward velocity [circles in Fig. 5(b)], respectively. The inset is the enlargement of the corresponding part of Fig. 5(b). If we assume $r(t) \equiv r = 0$ during the interaction process, we can similarly obtain the distribution formula of the longitudinal outgoing velocity of Rydberg atoms whose

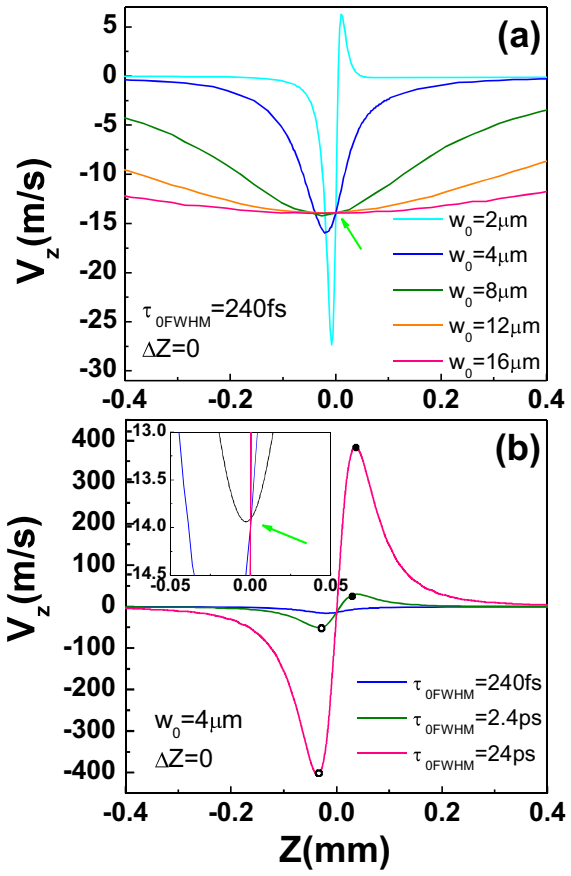

FIG. 5. Final outgoing longitudinal velocity distribution of excited ^{4}He atoms at positions along the z axis, where the simulation parameters are $\Delta Z = 0$; (a) $\tau_{0\mathrm{FWHM}} = 240$ fs, and $w_0 = 2,\ 4,\ 8,\ 12,\ 16\,\mu\mathrm{m}$; (b) $w_0 = 4\,\mu\mathrm{m}$, and $\tau_{0\mathrm{FWHM}} = 24$ ps, 2.4 ps, 240 fs. The other parameters are $I_0 = 2.8 \times 10^{15}\,\mathrm{W/cm^2}$ and $\lambda = 0.814\,\mu\mathrm{m}$.

initial positions are along the z axis under the condition of $\Delta Z = 0$ [17]:

$$v_{\parallel} = \frac{q^2 I_0}{1.33 \times 10^{-3} M m \omega^2} \left\{ \frac{z\sqrt{\pi}\tau}{k_0^2 w(z)^4} - \frac{1}{4c[1 + (z/Z_R)^2]} \right\}. \tag{11}$$

From Eq. (11) we can easily find that when $z_0 = 0$, the longitudinal outgoing velocity of the particles is a negative constant $V_{z,z_0=0}$ which is independent of w_0 and $\tau_{0\mathrm{FWHM}}$. For the laser intensity adopted by us, $V_{z,z_0=0} \approx -13.87\,\mathrm{m/s}$. If this formula is valid for our simulation, the lines plotted in Fig. 5 must pass through the same point ($z_0 = 0$, $V_z = V_{z,z_0=0}$). Indeed the lines obtained from the simulation do pass through the same point within the permissible range of error, as marked by the arrow in Fig. 5. According to Eq. (11), the longitudinal outgoing velocity increases with increasing pulse duration. Particularly, for a stable optical field ($\tau \to \infty$), the longitudinal outgoing velocity will reach infinity ($V_z \to \infty$). Apparently, this is unreasonable. Figure 6 presents the variation of longitudinal outgoing velocity, maximum forward velocity, and maximum backward velocity with

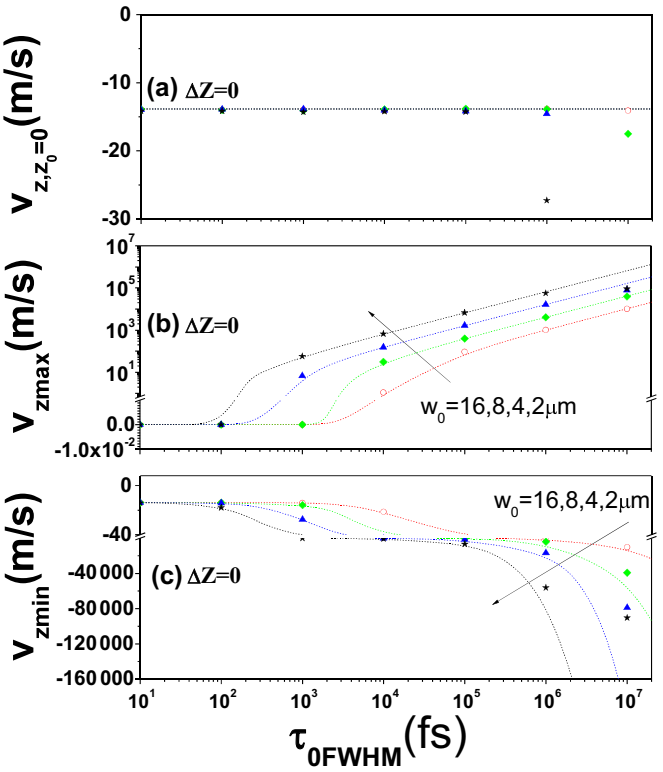

FIG. 6. (a) Variation of the outgoing longitudinal speed $V_{z,z_0=0}$ of the excited ^{4}He atoms with respect to laser pulse length $\tau_{0\mathrm{FWHM}}$ for $x_0 = y_0 = z_0 = 0$ and $\Delta Z = 0$. (b) Variation of the outgoing longitudinal forward maximum speed $V_{z\max}$ via $\tau_{0\mathrm{FWHM}}$ for $x_0 = y_0 = 0$ and $\Delta Z = 0$. (c) Same as (b) but for longitudinal backward maximum speed $V_{z\min}$. The dotted lines are for the results from Eq. (11) and the scattered symbols are for the simulation results. The other parameters are the same as those in Fig. 3.

respect to pulse length $\tau_{0\mathrm{FWHM}}$ [the dotted lines are for the results from Eq. (11), while the scattered symbols are for the simulation results]. It is evident that when $\tau_{0\mathrm{FWHM}} < 100$ ps, the simulation consequences match well with the formula, but when $\tau_{0\mathrm{FWHM}} > 100$ ps, the particles already move away from the center axis ($r \neq 0$), similarly as shown in Fig. 4(d), and this situation does not satisfy the derivation conditions of Eq. (11).

TABLE I. Maximum final radial speeds $V_{r\max}$ and longitudinal speeds $V_{z\min}$ of ^{1}H, ^{4}He, and ^{12}C Rydberg atoms with $\Delta Z = 0$ and $2c\tau_0$; other parameters are the same in all cases: $\tau_{0\mathrm{FWHM}} = 50$ ps, $w_0 = 2\,\mu$m.

	$a_0 = 0.0368$		$a_0 = 0.1$	
	$\Delta Z = 2c\tau_0$	$\Delta Z = 0$	$\Delta Z = 2c\tau_0$	$\Delta Z = 0$
	$V_{r\max}$ (m/s)	$V_{z\min}$ (m/s)	$V_{r\max}$ (m/s)	$V_{z\min}$ (m/s)
^{1}H	1.76×10^5	-1.34×10^4	4.32×10^5	-9.93×10^4
^{4}He	4.49×10^4	-3.38×10^3	2.38×10^5	-2.50×10^4
^{12}C	3.06×10^4	-1.13×10^3	1.34×10^5	-8.32×10^3

H and C are the main elements of an organism; hence, protons and carbon ions are now being used to treat cancer at a number of places around the world [20]. Therefore we may as well select H and C as operation examples using our above-mentioned method. Table I shows the maximum final speeds (longitudinal and radial) of a ^{4}He, lighter ^{1}H, and heavier ^{12}C atoms with one electron in the Rydberg state driven by a stronger laser pulse with $a_0 = 0.1$. For comparison, the simulation results with $a_0 = 0.0368$ are also listed in Table I. The longitudinal velocity can have different signs (positive for forward and negative for backward); however, only negative values are shown in the table. It should be noted that heavier excited atoms could endure stronger radial ponderomotive repulsive force, which means we can use a longer laser pulse to obtain an optimal acceleration.

IV. SUMMARY AND DISCUSSION

In summary, we simulated the Rydberg atoms accelerated in tightly focused laser fields with a high-order corrected optical description. The simulation results show that a laser pulse with a long pulse duration and a small waist favors the acceleration of Rydberg atoms. Some characteristics of acceleration were investigated. Lighter atoms (e.g., ^{1}H) are more easily pushed forward or pulled backward. In addition, this method can also be used to accelerate positive ions provided that at least one electron of the ion is in the Rydberg state. Because positive ions are more stable than neutral atoms, they can survive in the stronger laser fields; hence, positive ions can be accelerated to much higher speeds. However, this drag-acceleration mechanism will fail if all the electrons are ionized. It is noteworthy that the ratio of the excited neutral atoms over the ionized atoms also depends strongly on the laser intensity [19,21]. In certain situations, the ionization probability of a particle may decrease as laser intensity increases; i.e., intense laser fields can enhance the stabilization of the particles [22]. However, so far this has not been demonstrated experimentally, except for the atoms initially prepared in the Rydberg state [23]. On the other hand, Rydberg atoms have been observed to survive in the intense laser fields whose field amplitudes exceed the thresholds for static field ionization by more than six orders of magnitude [24]. If laser beams are focused to subwavelength waist radius [20], this method may be able to accelerate a Rydberg atom to much higher energies. In addition, we must be concerned about whether the Rydberg state can survive (may be ionized or destimulated) during such a long process. We recently adopted the calculation method provided in Ref. [25] and our results show that, under special conditions, the lifetimes of some Rydberg atoms in a strong field are very long.

ACKNOWLEDGMENTS

This work is partly supported by Natural Science Foundation of Shanghai (Grants No. 15ZR1411300 and No. 17ZR1402700).

[1] M. Gupta and D. Herschbach, J. Phys. Chem. A **105**, 1626 (2001).
[2] J. J. Gilijamse, S. Hoekstra, S. Y. T. van de Meerakker, G. C. roenenboom, and G. Meijer, Science **313**, 1617 (2006).
[3] L. Scharfenberg, S. Y. T. van de Meerakker, and G. Meijera, Phys. Chem. Chem. Phys. **13**, 8448 (2011).
[4] U. Eichmann, T. Nubbemeyer, H. Rottke, and W. Sandner, Nature **461**, 1261 (2009).
[5] C. Maher-McWilliams, P. Douglas, and P. F. Barker, Nat. Photon. **6**, 386 (2012).
[6] R. Rajeev, T. Madhu Trivikram, K. P. M. Rishad, V. Narayanan, E. Krishnakumar, and M. Krishnamurthy, Nat. Phys. **9**, 185 (2013).
[7] Q. Z. Xia, L. B. Fu, and J. Liu, Phys. Rev. A **87**, 033404 (2013).
[8] X. Cai, J. Zheng, and Qiang Lin, Phys. Rev. A **87**, 043401 (2013).
[9] D. P. Higginson, J. M. McNaney, D. C. Swift, G. M. Petrov, J. Davis, J. A. Frenje, L. C. Jarrott, R. Kodama, K. L. Lancaster, A. J. Mackinnon, H. Nakamura, P. K. Patel, G. Tynan, and F. N. Beg, Phys. Plasma **18**, 100703 (2011).
[10] A. Rakonjac, A. B. Deb, S. Hoinka, D. Hudson, B. J. Sawyer, and N. Kjærgaard, Opt. Lett. **37**, 1085 (2012).
[11] T. W. B. Kibble, Phys. Rev. Lett. **16**, 1054 (1966).
[12] P. X. Wang, S. Kawata, and Y. K. Ho, Opt. Express **18**, 14144 (2010).
[13] B. Quesnel and P. Mora, Phys. Rev. E **58**, 3719 (1998).
[14] M. P. de Boer and H. G. Muller, Phys. Rev. Lett. **68**, 2747 (1992).
[15] F. Morales, M. Richter, S. Patchkovskii, and O. Smirnova, Proc. Natl. Acad. Sci. USA **108**, 16906 (2011).
[16] Q. Wei, P. X. Wang, S. Kais, and D. Herschbach, Chem. Phys. Lett. **683**, 240 (2017).
[17] P. X. Wang, Q. Wei, P. Cai, J. X. Wang, and Y. K. Ho, Opt. Lett. **41**, 230 (2016).
[18] J. P. Barton and D. R. Alexander, J. Appl. Phys. **66**, 2800 (1989).
[19] T. Nubbemeyer, K. Gorling, A. Saenz, U. Eichmann, and W. Sandner, Phys. Rev. Lett. **101**, 233001 (2008).
[20] Y. I. Salamin, Z. Harman, and C. H. Keitel, Phys. Rev. Lett. **100**, 155004 (2008).
[21] A. Wójcik, R. Parzyński, and A. Grudka, Phys. Rev. A **55**, 2144 (1997).
[22] J. H. Eberly and K. C. Kulander, Science **262**, 1229 (1993).
[23] M. P. de Boer, J. H. Hoogenraad, R. B. Vrijen, R. C. Constantinescu, L. D. Noordam, and H. G. Muller, Phys. Rev. A **50**, 4085 (1994).
[24] U. Eichmann, A. Saenz, S. Eilzer, T. Nubbemeyer, and W. Sandner, Phys. Rev. Lett. **110**, 203002 (2013).
[25] M. Klaiber and D. Dimitrovski, Phys. Rev. A **91**, 023401 (2015).